J Mol Model (2013) 19:893–904
DOI 10.1007/s00894-012-1621-y

ORIGINAL PAPER

# Density functional conformational study of 2-O-sulfated 3,6 anhydro-α-D-galactose and of neo-κ- and ι-carrabiose molecules in gas phase and water

**Noreya Bestaoui-Berrekhchi-Berrahma · Philippe Derreumaux · Majda Sekkal-Rahal · Michael Springborg · Adlane Sayede · Noureddine Yousfi · Abd-Ed-Daim Kadoun**

Received: 29 May 2012 / Accepted: 1 October 2012 / Published online: 20 October 2012


**Abstract** We examined the conformational preferences of the 2-O-sulfated-3,6-α-D-anhydrogalactose (compound I) and two 1,3 linked disaccharides constituting-κ or ι-carrageenans using density functional and ab initio methods in gas phase and aqueous solution. Systematic modifications of two torsion angles leading to 324 and 144 starting geometries for the compound I and each disaccharide were used to generate adiabatic maps using B3LYP/6-31G(d). The lower energy conformers were then fully optimized using B3LYP, B3PW91 and MP2 with several basis sets. Overall, we discuss the impact of full relaxation on the energy and structure of the dominant conformations, present the performance comparison with previous molecular mechanics calculations if available, and determine whether our results are impacted, when polarization and diffuse functions are added to the 6-31G(d) basis set, or when the MP2 level of theory is used.

**Keywords** Adiabatic maps · Conformers · DFT methods · Full optimization · Gas and solvent · 2-O-sulfated-3,6-α-D-anhydrogalactose · Neo-κ-carrabiose · Neo-ι-carrabiose

**Electronic supplementary material** The online version of this article (doi:10.1007/s00894-012-1621-y) contains supplementary material, which is available to authorized users.

N. Bestaoui-Berrekhchi-Berrahma · M. Sekkal-Rahal (✉) · N. Yousfi · A.-E.-D. Kadoun
L2MSM, Faculté des Sciences,
Université Djillali Liabes de Sidi Bel Abbes,
B.P. 89, 22000 Sidi Bel Abbes, Algeria
e-mail: majsekkal@msn.com

P. Derreumaux
Laboratoire de Biochimie Théorique, CNRS, UPR 9080,
Université Paris Diderot, Sorbonne Paris Cité,
IBPC, 13, rue Pierre et Marie Curie,
75005 Paris, France

P. Derreumaux
Institut Universitaire de France,
103 Boulevard Saint-Michel,
75005 Paris, France

M. Springborg
Physikalische und Theoretische Chemie,
Universitaet des Saarlandes,
Postfach 15 11 50,
Saarbruecken 66041, Germany

A. Sayede
UCCS-CNRS UMR 8181, Faculté des Sciences de Lens,
Université d'Artois,
Rue, Jean-Souvraz SP-18,
Lens 62300, France

## Introduction

Carrageenans, which are found in the cell walls of numerous red seaweeds (Rhodophyta), are high-molecular-weight polysaccharides made up of repeating galactose units and 3,6-anhydro-α-D-galactose, both sulfated and nonsulfated. The units are joined by alternating α(1→3) and β(1→4) linkages [1–3]. Besides their wide applications in the food industry as thickening and gelling agents [4], chemically modified carrageenans can also lead to prototypes with potential medical interest for several diseases such as herpes, human papillomavirus (HPV) and AIDS [4].

Since the function of polysaccharides depend on their equilibrium conformations in the selected environment [2], the energy landscape of mono-, di- and trisaccharides has been subjected to energy minimizations and molecular

dynamics (MD) simulations in gas phase or in water using all-atom molecular mechanics (MM) force fields such as MM3, Tripos, CHARMM and GROMOS [3–34]. More recently, ab initio and density functional theory (DFT) calculations have been performed [5, 35–45] and DFT calculations at the B3LYP/6-311++G** [24, 35, 46–50] and B3LYP/6-31G** [51] levels of theory have shown to give reliable energies and geometries for several carbohydrates [24, 35, 46–50]. Vibrational frequencies of carbohydrates were also calculated using MM and spectroscopic force fields [52–54] and from 27 ps DFT MD simulations [55].

The aim of this work was to determine the preferred conformations of three carbohydrates in gas phase and water which have never been subjected to DFT calculations. These molecules, shown in Fig. 1, include the 2-O-sulfated-3,6-α-D-anhydrogalactose (compound I), the 4-O-sulfated 3,6-anhydro-α-D-galactopyranosyl(1→3)β-D-galacto-pyranose also called neo-κ-carrabiose (compound II) and the 4-O-sulfated 3,6-anhydro-α-D-galactopyranosyl(1→3)2-O-sulfated-β-D-galactopyranose or neo-κ-carrabiose (compound III).

To this end, we followed the procedure that we used for κ-carrabiose, characterized by a 1→4 linked disaccharide in carrageenans [56]. Note that neo-κ-carrabiose is the other κ-carrageenan constituting disaccharide with a 1→3 glycosidic linkage between the 4-O-sulfated 3,6-anhydro-α-D-galactopyranosyl and the β-D-galactopyranose units. Specifically, we first determined the conformational maps at the B3LYP/6-31G(d) level by systematically varying and constraining the two dihedral angles of the glycosic linkage for each disacharride and of the pyranose ring for compound I, while relaxing the other degrees of freedom. A total of 324 and 144 geometries were thus energy-minimized for compound I and each disaccharide, respectively. The lower energy conformers were then fully optimized using B3LYP, B3PW91 and MP2 with several basis sets and subsequently subject to normal mode analysis to guarantee they are actually minima on the potential energy surface and not transition states. This whole process was repeated for each molecule using the Onsager model to simulate the effect of solvent [57–60].

Details of the calculations are given in Computational details and nomenclature. For each disaccharide, we have selected the three 6-31G(d), 6-31G(d,p) and 6-31+G(d,p) basis sets coupled to the B3LYP and B3PW91 density functions and the single 6-31G(d) basis set coupled to MP2. For compound I, we also considered the 6-31G(d), 6-31+G(d) and 6-311++G(d,p) basis sets coupled to B3LYP and B3PW91. Our selection for the basis sets and methods was motivated by three reasons.

First, while B3LYP is the most commonly used functional in sugar field [5, 24, 35, 36, 38–40, 50], a recent study has shown that B3LYP functional is not the most appropriate for

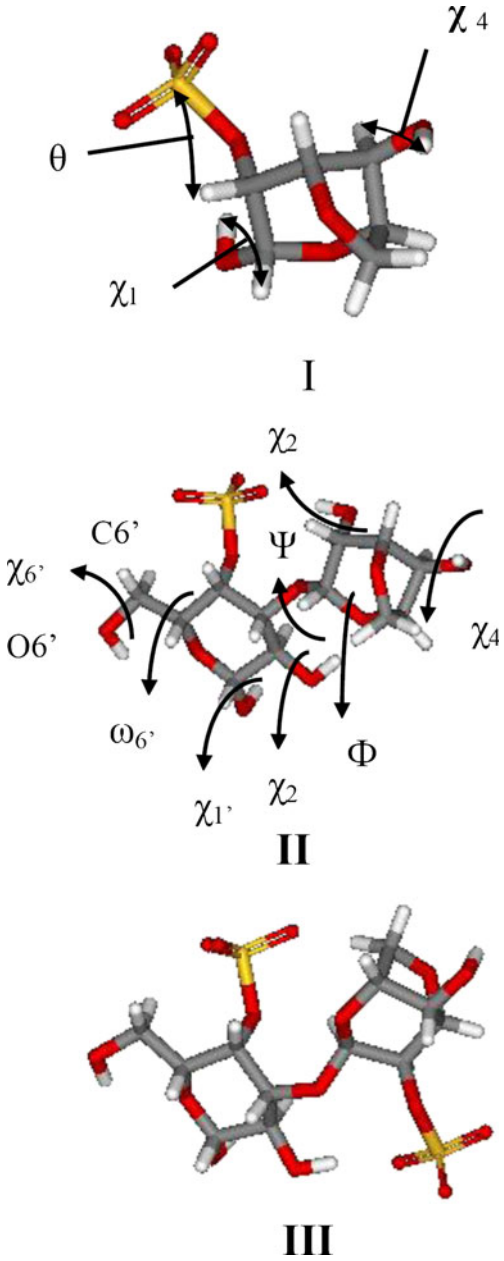


**Fig. 1** a- Structure of 2-O-sulfated-3,6-α-D-anhydrogalactose, dihedral angles θ and $\chi_1$ around the exocyclic angles of the hydroxymethyl group and hydroxyls groups (compound I), b- Structure of 1,3 linked disaccharide constituting κ-carrageenans, dihedral angles Φ and Ψ around the glycosidic linkage and exocyclic angles of the hydroxymethyl group and hydroxyls groups (compound II), c- Structure of 1,3 linked disaccharide constituting ι-carrageenans (compound III)

conformational studies, and B3PW91 gives better results [61]. However, B3PW91 is still mostly restricted to the study of well-defined conformers [30]. We recall that one important difference between B3LYP and B3PW91 is that B3LYP does not respect the uniform electron gas limit, while B3PW91 does [61].

Second, in addition to the standard 6-31G(d) and 6-31+G(d) basis sets for disaccharides [61], we tested the B3LYP/6-

311++G(d,p) and B3PW91/6-311++G(d,p) functionals and basis sets [35, 36, 50, 56] to determine whether our results are impacted when polarization or diffuse functions are added to the 6-31G(d) basis set [56]. Third, we wanted to determine what improvement in data quality is seen when the MP2 [30, 62] level of theory is used. Results and discussion reports the adiabatic maps of each compound and compares the DFT and MP2 fully relaxed, lower potential energy conformations both in gas phase and aqueous solution. The performance comparison with experiments and previous MM calculations, if available, is included and we also compare the DFT more physically relevant free energies with rotational, translational and vibrational corrections at 298 K in gas phase.

## Computational details and nomenclature

The conformational space of carbohydrates is generally described by the dihedral angles Φ and Ψ of the glycosidic linkage. Following the IUPAC recommendations [63], we used for the two disaccharides, Φ=O5-C1-O1-C3' and Ψ= C1-O1-C3'-C4', the primes associated with the atoms of the non reducing sugar unit (Fig. 1b and c). For compound I, we used the dihedral angles of the pyranose cycle: θ=H(2)–C2–O2-S(O)2 and $\chi_1$=H(1)–C1–O1–H(O)1) (Fig. 1a).

The initial structures of the three compounds were taken from the crystal hexa-í-carrageenan double helix conformation [64], because it has 1→3 glycosidic linkages. Crystal data exist for κ-carrabiose, but these report conformations with 1→4 linkages [65, 66]. From this double helix, we took the monosaccharide conformation for compound I and the disaccharide conformation for compounds II and III and further eliminated the sulfate atom at position C2 for compound III. These conformations, after full optimization using B3LYP/6-31G(d) in gas phase, are characterized by (θ, $\chi_1$) values of (36°, −68°) for compound I and (Φ, Ψ) values of (55°,53°) and (33°,61°) for compounds II and III, and have TT, EggGGT and EggGT configurations for the exocyclic groups in compounds I, II and III, respectively.

Each resulting optimized structure was then used as starting geometries for all geometry modifications required to generate the conformer libraries of the molecule by rigid rotations of the dihedral angles Φ and Ψ for compounds II and III, and the dihedral angles θ and $\chi_1$ for compound I as described in ref. 36. Following French and Dowd [67] recommendations, the adiabatic maps of compounds II and III were built by varying each dihedral angle by increments of 30 °, resulting in a total of 144 conformations. Due to its reduced number of degrees of freedom, the map of compound I was generated by varying each dihedral angle by increments of 20 °, resulting in a total of 324 conformations. Once the set of Φ and Ψ angles for compounds II and III was selected, (or θ and $\chi_1$ for compound I), these angles were kept frozen while optimizing all other degrees of freedom [56]. Among all minima identified on the adiabatic maps, only the lower energy minima were fully optimized in gas phase at the B3LYP/6-31G(d), B3LYP/6-31G(d,p), B3LYP/6-31+G(d), B3PW91/6-31G(d), B3PW91/6-31G (d,p), B3PW91/6-31+G(d) and MP2/6-31G(d) levels for each compound. For compound I, we also performed full optimizations using B3LYP/6-311++G(d,p) and B3PW91/6-311++G(d,p).

The same procedure was carried out for the three compounds by simulating the presence of water using the Onsager model [68]. In this model, the solute is placed in a spherical cavity inside the solvent, which is described as a homogeneous polarizable medium of dielectric constant [69], set to 78 for water [29]. Using all conformers prior to optimization, the *volume* algorithm in Gaussian program yields an average cavity radius of 4.6 Å for compound I, 5.5 Å for compound II and 5.7 Å for compound III. After full optimization in solvent using B3LYP/6-31G(d), the starting (θ, $\chi_1$) values are (29°,−67°) for compound I, and the starting (Φ,Ψ) values are (1°,132°) and (45°,59°) for compounds II and III. Finally, the adiabatic maps were calculated and full relaxation of the lower energy minima was performed with the procedure used for gas phase. It is important to note that all calculations on compounds II and III did not consider the rotation around the C-O or S-O bonds of the sulfate group.

All calculations were carried out with the Gaussian 03 program (version 6.0, revision B.03) [70]. Results were explored using the Gaussview software and the maps drawn with the Surfer software [71]. Optimization was considered satisfactory using the tight condition (RMS force criterion of $1*10^{-5}$) for the adiabatic maps and the very tight condition (RMS force criterion of $1*10^{-6}$) along with the absence of negative vibrational frequencies for the fully relaxed conformations.

In addition to the glycosidic torsional angles, we examined other variables to assess the conformations. The orientations of the hydroxymethyl groups are characterized by the torsional angles ω' and $\chi_6$, defined by the atoms O5'-C5'-C6'-O6' and C5'-C6'-O6'-H6 [7], respectively (Fig. 1a and b). Their rotamers are referred to [72] as *gauche-trans* (*gt*), *gauche-gauche* (*gg*) or *trans-gauche* (*tg*), corresponding to ω values of 60°, −60° and 180°, respectively. The orientation of the hydroxyl hydrogens [73] is indicated by the torsional angles $\chi_n$ defined by the atoms H(n)–Cn–On–H(O)n (Fig. 1a and b). Their values are described by a one-letter code [74]: S for angles between −30° and +30°, g for angles between 30–80°, T for angles with an absolute value larger than 150°, G for angles between −30° and −80°, and E for angles between −80° and −150°.

## Results and discussion

2-O-sulfated-3,6-α-D-anhydrogalactose (compound I)

*Adiabatic map in gas phase*

The map using B3LYP/6-31G(d) and a 18×18 grid is shown in Fig. 2a, with the contour line values in kcal/mol with respect to the lowest energy point. There are three minima, designated as A, B and C according to their (θ, $\chi_1$) values: A at (−24°,152°), B at (56°,152°) and C at (−64°,32°). Their energies are 0, 2.1 and 3.4 kcal/mol, respectively.

Several computational studies have focused on the configuration of the ring in monosaccharides. These works on glucose and its epimers, methyl 3,6-anhydro-α-galactopyranoside, β-D-galactopyranose, α-D-galactopyranose, β-D-allopyranose and β-D-glucopyranoside units in gas phase have revealed minima with either chair, boat or skew forms of the sugar ring [44, 54, 75–81]. Here, we find that A and B display a chair $^1C_4$ form, while C has a boat $B_{1,4}$ conformation. It is well established that hydrogen bonding (H-bond) constitutes a significant factor in determining relative energies and ring geometries in gas phase [43]. H-bond has also been shown to be prevalent in carbohydrate crystal structures with the hydroxyl groups, acting as both hydrogen bond donors and acceptors [82–84]. As shown in Fig. SI.1a (see supplementary data), the conformers A and C display one inter-residue H-bond between the oxygen of the sulfate group and the hydrogen of the neighboring hydroxyls (H(O1)), while conformer B is free of any H-bond.

Looking at the torsions angles of the secondary exocyclic hydroxyl groups ($\chi_1$ and $\chi_4$) we found they are TT for conformers A and B, and gT for C. All hydroxyl groups confined in dihedral $\chi_1$ have clockwise orientations in the three conformers while the hydroxyl groups confined in the dihedral $\chi_4$ have a counter clockwise orientation in conformer C.

*Adiabatic map in water*

The map using B3LYP/6-31G(d) is shown in Fig. 2b. There are three minima, designated as A, B' and C' with the following (θ, $\chi_1$) values: A at (−11°, 133°), B' at (28°, 173°) and C' at (9°, −167°). Their energies with respect to the lowest energy minimum are: 0, 1.55 and 3.19 kcal/mol, respectively. Comparing with the minima in gas phase, we find that the two lower energy minima remain nearly at the same places, but the location of the third state shifts substantially. The three minima adopt a chair $^1C_4$ conformation, while only two adopt this configuration in gas phase. From Fig. SI.2a (see supplementary data), we see that conformer A has one intra-residue H-bond between the oxygen belonging to the sulfate group and the hydrogen of the neighboring hydroxyls (H (O1)). In contrast, B' and C' do not contain any H-bond. Again, this finding runs in contrast with the gas phase results where two minima have one H-bond. The exocyclic torsion angles correspond to various conformations: TT for A and B' and ET for C'. In all conformers, the secondary exocyclic hydroxyl groups indicate clockwise orientations.

*Full optimization of the lower energy conformers in gas phase and water*

One problem of using small grids is that some low energy conformers can be missed between two points. The drawback of adiabatic map is that the energetics and the structural characteristics of the minima may vary upon full optimization. To this end, we have proceeded to full optimization of the three lower energy conformers using B3LYP and B3PW91 with 6-31G(d), 6-31G(d,p) and 6-31+G(d), as well as MP2/6-31G(d). The resulting minima in gas phase and aqueous solution are described in Tables 1 and 2, respectively.

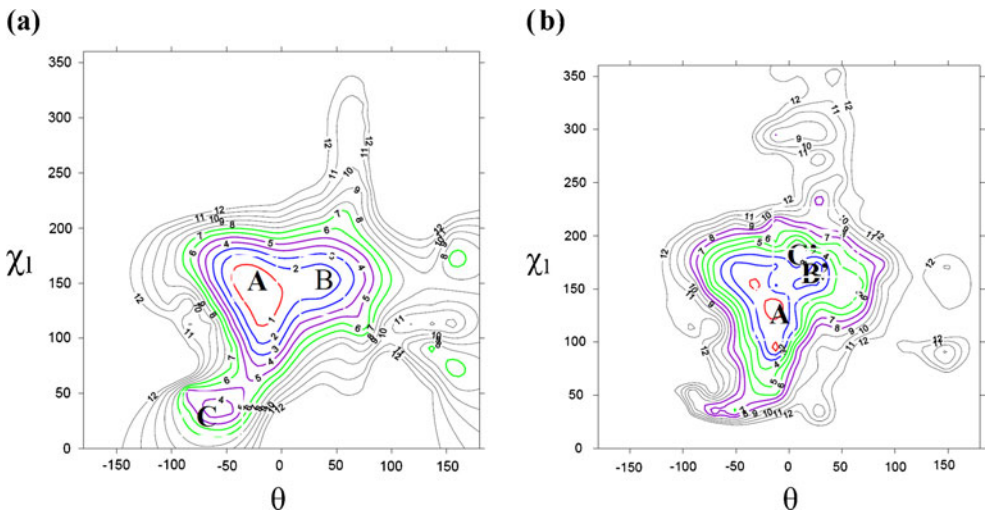


**Fig. 2** Relaxed iso-potential maps at the B3LYP/6-31G(d) level of compound I: **a** (map 2a) in the gas phase and **b** (map 2b) in water (ΔE in kcal/mol)

**Table 1** Relative energies and Gibbs free energies (kcal/mol), θ and $\chi_1$ torsions (°) of compound I in gas phase after full optimization with the B3LYP and B3PW91 methods and different basis sets and MP2/6-31G(d)

| Method conformer | B3LYP[a] | | | B3LYP[b] | | | B3LYP[c] | | | B3PW91[d] | | | B3PW91[e] | | | B3PW91[f] | | | MP2[g] | | |
|---|---|---|---|---|---|---|---|---|---|---|---|---|---|---|---|---|---|---|---|---|---|
| | A | B | C | A | B | C | A | B | C | A | B | C | A | B | C | A | B | C | A | B | C |
| ΔE | 0.00 | 1.26 | 1.52 | 0.00 | 0.64 | 1.70 | 0.00 | 0.40 | 1.83 | 0.00 | 1.27 | 1.66 | 0.00 | 0.75 | 1.80 | 0.00 | 0.57 | 1.95 | 0.00 | 0.42 | 1.68 |
| (θ, $\chi_1$) | −23, 144 | 31, 151 | −56, 55 | −21, 139 | 30, 151 | −55, 55 | −23, 140 | 33, 152 | −55, 54 | −21, 141 | 30, 151 | −56, 55 | −20, 137 | 30, 151 | −55, 54 | −22, 138 | 33, 152 | −56, 53 | −14, 138 | 26, 153 | −56, 54 |
| ΔG | 0.00 | 0.61 | 1.85 | 0.21 | 0.00 | 2.21 | 0.41 | 0.00 | 2.55 | 0.00 | 0.43 | 2.03 | 0.15 | 0.00 | 2.24 | 0.18 | 0.00 | 2.40 | 0.01 | 0.00 | 2.01 |

[a] B3LYP/6-31G(d),

[b] B3LYP/6-31+G(d),

[c] B3LYP/6-311++G(d,p),

[d] B3PW91/6-31G(d)

[e] B3PW91/6-31+G(d)

[f] B3PW91/6-311++G(d,p)

[g] MP2/6-31G(d)

**Table 2** Optimized conformations of compound I with their θ and $\chi_1$ torsional angles (°) and relative energies (kcal/mol) in water

| Method conformer | B3LYP[a] | | | B3LYP[b] | | | B3LYP[c] | | | B3PW91[d] | | | B3PW91[e] | | | B3PW91[f] | | |
|---|---|---|---|---|---|---|---|---|---|---|---|---|---|---|---|---|---|---|
| | A | B’ | C’ | A | B’ | C’ | A | B’ | C’ | A | B’ | C’ | A | B’ | C’ | A | B’ | C’ |
| ΔE | 0.54 | 0.96 | 0.00 | 1.68 | 1.16 | 0.00 | 1.75 | 1.13 | 0.00 | 2.29 | 2.63 | 0.00 | 1.55 | 1.13 | 0.00 | 1.67 | 1.18 | 0.00 |
| (θ, $\chi_1$) | −25, 149 | 21, 153 | 19, 153 | −23, 145 | 21, 155 | 20, 155 | −24, 146 | 24, 155 | 23, 156 | −24, 147 | 20,152 | 13, 152 | −22, 143 | 21, 154 | 20, 154 | −24, 144 | 24, 155 | 23, 155 |

[a] B3LYP/6-31G(d),

[b] B3LYP/6-31+G(d),

[c] B3LYP/6-311++G(d,p),

[d] B3PW91/6-31G(d)

[e] B3PW91/6-31+G(d)

[f] B3PW91/6-311++G(d,p)

Looking at the gas phase results in Table 1, we see that the potential energy ranking is conserved independently of the method and basis set used and follows A < B < C. The maximal ΔE between A and C ranges, however, from 1.5 (B3LYP/6-31G(d)) to 1.9 (B3PW91/6-311++G(d,p)) kcal/mol and that between A and B from 0.4 (MP2 and B3LYP/6-311++G(d,p)) to 1.3 kcal/mol (B3PW91 and B3LYP with 6-31G(d)). Similarly, the optimized θ and $\chi_1$ values of each conformer do not differ from one basis set to another, nor using B3LYP, B3PW91 and MP2. A is located at ~ (−23°, 140°), B at ~ (30°, 150°) and C at (−55°, 55°). Note there is a difference of ± 20° between the "adiabatic" and fully relaxed minima.

Including the entropy at 298 K changes the energy ordering of the structures. C still has the highest energy, but B has the lowest free energy except using B3PW91 and B3LYP with 6-31G(d). ΔG between A and B is very small, however, varying between 0.0 (MP2 and B3PW91 with 6-31G(d)) and 0.4 kcal/mol (B3LYP/6-311++G(d,p)).

The picture changes drastically from adiabatic to full optimizations in solvent. As shown in Table 2, the energy ranking follows C' < A and B', independently of the method used, and A is no longer the global potential energy minimum. C' is located at around (20°, 155°). B3LYP and B3PW91 with 6-31G(d) underestimate and overestimate the energy differences between the conformers, respectively (ΔE max of 0.9 and 2.6 kcal/mol). They also rank A < B'. In contrast, the four other calculations using B3LYP and B3PW91 with more complex basis functions converge to the same energy differences and rank B' < A. Interestingly, while the fully optimized conformers are located in three distinct (θ and $\chi_1$) basins in gas phase, they are located in only two basins in solvent: A is located at (−24°, 155°) and B' is at (21°, 155°) as C'. To explain why B' and C' have such close geometries in all calculations and differ by 1.1 kcal/mol using the more complex basis sets, we found that Ω1, the cyclic torsional angle O6-C5-C4-O(4), varies from −168° in B' to 84° in C'.

In an experimental study on models for glucose, the methyl 3,6-anhydro-β-D-glucopyranoside and methyl 3,6-anhydro-β-D-galactopyranoside were found in the $^4C_1$ and $B_{1,4}$ conformations in aqueous solution [85]. The application of the solvation model of Tomasi and co-workers [86] to QM calculations indicates that the chair form is stabilized by water in methyl 3,6-anhydro-β-D-galactopyranoside and 3,6-anhydro-α-D-galactopyranoside, but the boat form is stabilized by water in methyl 3,6-anhydro-β-D-glucopyranoside [87]. Here we found that the chair form is preferred in water with all three minima vs. two minima in gas phase displaying this conformation.

## Neo-κ-carrabiose (compound II)

### *Adiabatic maps in gas phase and water*

The resulting maps from 12×12 grids using B3LYP/6-31G (d) are shown in Fig. 3a-b. In gas phase, there are two minima with (Φ, Ψ) values of (85°, 113°) and (55°, 143°). Their relative energies are: 0.00 and 2.2 kcal/mol. The two conformers, E and F, are thus located in the same basin (Fig. 3a). For both minima, we find two inter-residue H-bonds (Fig. SII.1) (see supplementary data), all the hydroxyls groups on the galactopyranosyl and the 3,6-anhydro-α-D-galactopyranosyl units have clockwise orientations, and the exocyclic torsion angles for the non-reducing unit ($\chi_1$',$\chi_2$',$\omega_6$',$\chi_6$') have EggG configuration while those for the reducing unit ($\chi_2$,$\chi_4$) have GT configuration.

Table 3 also reports the results of adiabatic maps obtained by using several MM force fields and hard-sphere potentials in gas phase. We note that our lowest energy conformer, E at (85°, 113°), is close to the predictions using a hard-sphere potential (100°, 120°) [88], and an older version of the MM3 force field (80°,90°) [9]. In contrast, CHARMM25 (68°,72°) [22] and a more recent version of MM3 (86°,159°) [12] force fields failed to predict the conformer E as the ground state with Δψ

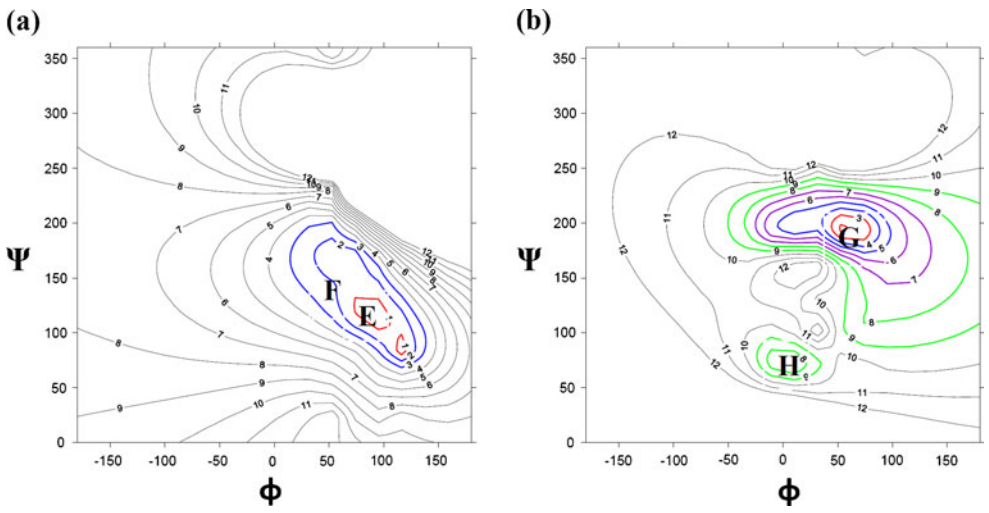


**Fig. 3** Relaxed iso-potential maps at the B3LYP/6-31G(d) level of compound II: **a** (map 3a) in the gas phase and **b** (map 3b) in water. (ΔE in kcal/mol)

**Table 3** Optimized conformations of compound II in gas phase with their relative energies and Gibbs free energies (kcal/mol) and Φ, Ψ angles (°)

| Method conformer | B3LYP[a] | | B3LYP[b] | | B3LYP[c] | | B3PW91[d] | | B3PW91[e] | | B3PW91[f] | | MP2[g] | | MM3[h] | | Fiber diffraction[i] | Modeling results[j] | CHARMM25[k] | | Tripos[l] | | HS[m] | MM3[n] |
|---|---|---|---|---|---|---|---|---|---|---|---|---|---|---|---|---|---|---|---|---|---|---|---|---|
| | E | F | E | F | E | F | E | F | E | F | E | F | E | F | 1st | GM | GM | GM | GM | 1st | GM | 1st | GM | GM |
| ΔE | 0.52 | 0.00 | 0.62 | 0.00 | 0.49 | 0.00 | 0.60 | 0.00 | 0.72 | 0.00 | 0.59 | 0.00 | 1.22 | 0.00 | 0.00 | 0.9 | | | 0.0 | 1.0 | 0.0 | 1.1 | | |
| (θ, ψ) | 92, 128 | 86, 113 | 93, 127 | 87, 111 | 91, 128 | 86, 116 | 93, 128 | 87, 113 | 94, 127 | 88, 110 | 92, 127 | 87, 115 | 94, 124 | 84, 109 | 86, 159 | 82, 96 | 82, 96 | 82, 96 | 68, 72 | 157, -56 | 80, 80 | −40, 90 | 100, 120 | 80, 90 |
| ΔG | 0.45 | 0.00 | 0.37 | 0.00 | 0.63 | 0.00 | 0.70 | 0.00 | 0.59 | 0.00 | 0.83 | 0.00 | | | | | | | | | | | | |

[a] B3LYP/6-31G(d)

[b] B3LYP/6-31G(d,p)

[c] B3LYP/6-31+G(d)

[d] B3PW91/6-31G(d)

[e] B3PW91/6-31G(d,p)

[f] B3PW91/6-31+G(d)

[g] MP2/6-31G(d)

[h] MM3 analysis (ref. 12)

[i] Fiber diffraction analysis (ref. 7, 64)

[j] (ref. 7, 9, 22)

[k] (ref. 22)

[l] (ref. 7)

[m] Hard-sphere method (ref. 88)

[n] (ref. 9)

GM and 1st stand for the global and first excited energy minima

**Table 4** Optimized conformations of compound II in water with their relative energies (kcal/mol) and Φ, Ψ angles (°)

| Method conformer | B3LYP[a] | | B3LYP[b] | | B3PW91[c] | | B3PW91[d] | |
|---|---|---|---|---|---|---|---|---|
| | G | H | G | H | G | H | G | H |
| ΔE | 0.00 | 13.38 | 0.00 | 6.63 | 0.00 | 11.73 | 0.00 | 9.66 |
| (θ, ψ) | 87, 147 | −50, 114 | 85, 144 | 1, 124 | 88, 148 | 5, 129 | 86, 146 | 3, 123 |

[a] B3LYP/6-31G(d)

[b] B3LYP/6-31+G(d)

[c] B3PW91/6-31G(d)

[d] B3PW91/6-31+G(d)

deviations of 40° and the Tripos force field finds (80°,80°) [7]. Also note that the first excited state predicted by CHARMM25 and Tripos differs substantially from the F conformer.

Looking at the adiabatic map in solvent (Fig. 3b), we also find two minima with (Φ, Ψ) of (61°, −168°) and (31°, 72°). Their relative energies are: 0. and 8.7 (kcal/mol). Only, the lowest energy conformer, G, has two inter-residue H-bonds (Fig. SII.2) (see supplementary data) and all hydroxyls groups on the galactopyranosyl and the 3,6-anhydro-α-D-galactopyranosyl units with clockwise orientations.

*Full optimization in gas phase and water*

We have proceeded to full optimizations of the low energy conformers using B3LYP and B3PW91 with 6-31G(d) and 6-31+G(d) in both environments. MP2 with 6-31G(d) and B3LYP and B3PW91 with 6-31G(d,p) were also used in gas phase. The resulting minima are described in Tables 3 and 4, respectively.

Looking at the gas phase results in Table 3, the global potential energy minimum (F) is found at ~ (87°, 111°) and the second minimum (E) is located at ~ (92°, 126°) independently of the method and basis set used. Thus we have a different energy ranking with the gas phase results under the adiabatic approximation. The energy difference between F and E is, however, method-dependent, on the order of 0.5–0.7 kcal/mol using B3LYP and B3PW91 with various basis sets vs. 1.2 kcal/mol using MP2. We note that our lowest energy conformer, F, is very close to the fiber diffraction values with (ΔΦ, ΔΨ) of (5°, 15°) and is independent of the inclusion of polarization or diffuse functions using both B3LYP and B3PW91. We also note that including the entropy at 298 K does not change the energy ordering of the two structures and marginally impacts the conformational distribution in all the calculations.

The results in Table 4 show that in water the location of the lowest potential energy minimum, G, shifts upon full relaxation from (61°, −168°) to (85°, 144°) in the four calculations. The relative energy and the position of the minimum H are method-dependent. H is located around (3°, 125°) by three calculations vs. (−50°, 114°) using B3LYP/6-31G(d). The relative energy of H varies between 6.6 and 13.4 kcal/mol using B3LYP and between 9.6 and 11.7 kcal/mol using B3PW91. Irrespective of the method, the Boltzmann population of H state is therefore equal to zero in aqueous solution at room temperature.

The exocyclic torsional angles for conformer G with the B3LYP and B3PW91 methods and the 6-31G(d) or 6-31+G(d)

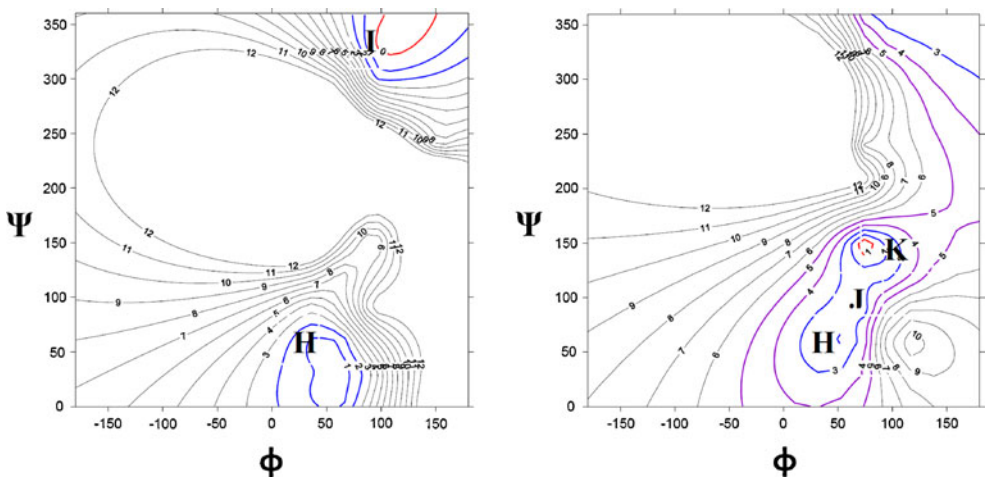


**Fig. 4** Relaxed iso-potential maps at the B3LYP/6-31G(d) level of) compound III: **a** (map 4a) in the gas phase and **b** (map 4b) in water. (ΔE in kcal/mol)

**Table 5** Optimized conformations of compound III in gas phase with their energies and Gibbs free energies (kcal/mol) and Φ, Ψ torsions (°)

| Method conformer | B3LYP[a] | | B3LYP[b] | | B3LYP[c] | | B3PW91[d] | | B3PW91[e] | | B3PW91[f] | | MP2[g] | | MM3[h] | | CHARMM[i] | | Tripos[j] | | HS[k] | HS[l] |
|---|---|---|---|---|---|---|---|---|---|---|---|---|---|---|---|---|---|---|---|---|---|---|
| | I | H | I | H | I | H | I | H | I | H | I | H | I | H | 1st | GM | GM | 1st | GM | 1st | GM | GM |
| ΔE | 0.00 | 1.03 | 0.00 | 0.90 | 0.00 | 0.05 | 0.00 | 0.41 | 0.00 | 0.31 | 0.43 | 0.00 | 0.00 | 0.46 | 0.4 | 0.0 | 0.0 | 2.1 | 0.0 | 0.5 | - | - |
| (θ, ψ) | 95, −27 | 33, 62 | 100, −34 | 34, 61 | 99, −35 | 36, 61 | 95, −25 | 36, 62 | 97, −27 | 36, 61 | 94, −27 | 37, 61 | 89, −21 | 30, 63 | 89, 165 | 72, 87 | 42, 54 | 153, 63 | 60, 75 | −30, 90 | 70, 80 | 70, 95 |
| ΔG | 0.00 | 0.26 | 0.00 | 0.70 | 2.54 | 0.00 | 0.12 | 0.00 | 0.00 | 0.03 | 0.00 | 1.38 | | | | | | | | | | |

[a] B3LYP/6-31G(d)

[b] B3LYP/6-31G(d,p)

[c] B3LYP/6-31+G(d)

[d] B3PW91/6-31G(d)

[e] B3PW91/6-31G(d,p)

[f] B3PW91/6-31+G(d)

[g] MP2/6-31G(d)

[h] MM3analysis (ref. 12)

[i] (ref. 23)

[j] (ref. 7)

[k] Hard-sphere method (ref. 64)

[l] Hard-sphere method (ref. 88)

**Table 6** Optimized conformations of compound III in water with their energies (kcal/mol) and Φ, Ψ torsions (°)

| Method conformer | B3LYP[a] | | | B3LYP[b] | | | B3PW91[c] | | | B3PW91[d] | | | CHARMM[e], ε=80 | |
|---|---|---|---|---|---|---|---|---|---|---|---|---|---|---|
| | H | J | K | H | J | K | H | J | K | H | J | K | GM | 1st |
| ΔE | 0.50 | 0.73 | 0.00 | 0.00 | 1.20 | 4.56 | 1.31 | 2.29 | 0.00 | 0.00 | 0.77 | 0.13 | 0.0 | 0.5 |
| (θ, ψ) | 44, 59 | 68,121 | 98, 156 | 54, 72 | 69, 122 | 94, 151 | 48, 63 | 68.121 | 98, 156 | 50, 69 | 68.121 | 95, 152 | 60, 66 | 173, 140 |

[a] B3LYP/6-31G(d),

[b] B3LYP/6-31+G(d),

[c] B3PW91/6-31G(d)

[d] B3PW91/6-31+G(d)

[e] (ref. 23)

basis sets are in a GggGGT configuration. They differ slightly from the values with B3LYP/6-31G(d), EggGGT. The exocyclic torsional angles for conformer H have a GggGgT configuration in all calculations.

Neo-ι-carrabiose; (compound III)

*Adiabatic maps in gas phase and aqueous solution using 12× 12 grids*

From the adiabatic map in gas phase using B3LYP/6-31G(d) and shown in Fig. 4a, there are two minima with (Φ, Ψ) values close to (93°, −29°) for I and (33°, 61°) for H. Their relative potential energies are: 0.00 and 0.96 kcal/mol, respectively. Only I has one H-bond between the oxygen belonging to the sulfate group and the hydrogen of one of the neighboring hydroxyl groups O(S)-… H'(O'2) (Fig. SIII.1) (see supplementary data). The orientations of the primary and secondary exocyclic hydroxyl groups in the two conformers through the dihedrals ($\chi_{1'}$, $\chi_{2'}$, $\omega_{6'}$, $\chi_{6'}$) and $\chi_4$ are EggG and T, respectively. The hydroxyls on the galactopyranosyl and the 3,6 anhydro-α-D-galactopyranosyl units have clockwise orientations. As seen in Table 5, adiabatic maps in gas phase with CHARMM [23], Tripos [7], MM3 [12] and hard-sphere calculations [64, 88] all point to a global minimum around the H state, and a first excited state to different regions, (89°, 165°) by MM3, (153, 63°) by CHARMM and (−30°, 90°) by Tripos.

From our adiabatic map in aqueous solution (Fig. 4b), we find three low energy conformers: H at (45°, 59°), J at (75°, 119°) and K at (105°, 149°). Their relative energies are: 0, 1.15 and 1.6 kcal/mol, respectively. Note that an adiabatic map using CHARMM force field and a dielectric constant of 80 [23] found a global minimum at (60°, 66°) near our conformer H (Table 6). The second CHARMM-predicted minimum at (173°, 140°) differs, however, substantially from our J and H conformers.

Examining the structures of our conformers in aqueous solution (Fig. SIII.2 in supplementary data), only the conformer J has one inter-residue H-bond. In the three conformers, the orientations of the primary and secondary exocyclic hydroxyl groups through the dihedrals ($\chi_{1'}$, $\chi_{2'}$, $\omega_{6'}$, $\chi_{6'}$) and $\chi_4$ are EggG and T, respectively, and all the hydroxyl groups on the galactopyranosyl and the 3,6-anhydro-α-D-galactopyranosyl units have clockwise orientations.

*Full optimization in gas phase and water*

The gas phase results in Table 5 shows there is almost no difference in the optimized (Φ, Ψ) values of the two conformers using B3LYP and B3PW91 combined with 6-31G (d) or 6-31G(d,p), with I, the global energy minimum, located at ~ (95°, −27°), H, the second minimum located at ~ (35°, 61°) and ΔE varying between 0.4 and 0.9 kcal/mol. Using 6-31+G(d), the positions of two minima do not change, but either they are equiprobable (ΔE of 0.05 kcal/mol with B3LYP) or I becomes the global minimum with an energy about 0.4 kcal/mol lower than that of H (B3PW91). Finally, using MP2/6-31G(d), both H and I remain at the same location, but I has an energy about 0.8 kcal/mol lower than that of H. Including the entropy at 298 K impacts both the energy ordering and distribution of the structures. Both I and H have very similar free energies using B3PW91 and B3LYP with 6-31G(d) and B3PW91/6-31G(d,p). H is, however, destabilized by 0.7 and 1.4 kcal/mol using B3LYP/6-31G(d,p) and B3PW91/6-31+G(d), respectively. In contrast, I is destabilized by 2.5 kcal/mol using B3LYP/6-31++G(d).

The results of full optimization in water are shown in Table 6. Using 6-31G(d), the energy ranking follows K < H < J with relative energy of (0., 0.5 and 0.7) with B3LYP vs. (0., 1.3 and 2.3) kcal/mol with B3PW91. K is located at (98°, 156°). In contrast, using 6-31+G(d), the energy ranking is H < J < K with relative energy of (0., 1.2 and 4.6) with B3LYP and the energy ranking is H < K < J with relative energy of (0., 0.1 and 0.8) kcal/mol with B3PW91. The addition of diffuse functions suggests that H, located near (50°, 70°), is likely the global energy minimum.

## Conclusions

The aim of this study was to determine the conformational preferences of 2-O-sulfated-3,6-α-D-anhydrogalactose, and the neo-κ- and neo-í-carrabiose molecules in gas phase and water. The choice of our molecules is relevant as these sulfated carbohydrate molecules are important components in the area of structural glycosciences, for which energetic information is quite sparse. To this end, we followed a two-step procedure: construction of adiabatic maps at B3LYP/6-31G(d) followed by full relaxation of the lower energy conformations using B3LYP, B3PW91 and MP2 levels of theory and several basis sets. Our results on the three compounds can be summarized as follows.

First, there is often a non-negligible deviation in the dominant fully-relaxed conformations from gas phase to water, and the potential energy landscape can change from adiabatic to full relaxation in both environments. The global minimum of neo-κ-carrabiose in water shifts from the adiabatic values of (61°, -168°) to the fully relaxed values of (85°, 144°) using four calculations. The three dominant states of neo-κ-carrabiose are located in three basins in gas phase vs. two in water and the global energy minimum of 2-O-sulfated-3,6-α-D-anhydrogalactose shifts from (−23°, 140°) in gas phase to (21°, 155°) in water. Whether the Onsager solvent model, which does not take into account the formation of hydrogen bonds between the carbohydrate molecule and water, likely to break internal hydrogen bonds, is responsible for this change from *in vacuo* to solvent remains to be determined. To clarify this aspect, we are repeating some calculations with explicitly present water molecules. This limitation of the Onsager model explains why we did not report free energies in solvent.

Second, full optimization using B3LYP and B3PW91 combined with our basis set has no impact on the structural characteristics and the potential energy ranking of the dominant conformations of 2-O-sulfated-3,6-α-D-anhydrogalactose and neo-κ-carrabiose in gas phase and water, and neo-í -carrabiose in gas phase. This is consistent with previous studies [61]. However, this observation does not hold for neo-í-carrabiose in solvent, at least with the Onsager model, where the ranking varies from 6-31+G(d) to 6-31G(d), i.e., by the addition of diffusion and polarization on heavy atoms to the 6-31G(d) basis set. We also note that the potential energy difference between the conformers and the position of the excited states change upon addition of one diffuse function to 6-31G(d), 6-31+G(d) and 6-311++G(d,p) for the three compounds.

Third, the MP2 level of theory does not much improve the quality of the gas phase data for the three compounds, although the potential energy difference between the two minima increases by 0.5 kcal/mol for neo-κ-carrabiose. In contrast, entropy corrections at 298 K impact the ordering of the conformers of compounds I and III, but not compound II in gas phase.

Finally, although the relevance of our DFT and MP2 results on the three carbohydrate molecules with respect to the complex physiological occurrence of the native polysaccharides remains to be determined, we find significant deviations with previous MM force field calculations on the two disaccharides, providing therefore reference values in gas phase for improving force fields that are currently used to decipher the structures and dynamics.

**Acknowledgments** N. B-B. B thanks D. J. Fox from his helpful suggestions to perform calculations and M. S-R thanks the Alexander von Humboldt foundation (Bonn) for grants

## References

1. Genicot-Joncour S, Poinas A, Richard O, Potin P, Rudolph B, Kloareg B, Helbert W (2009) Am Soc Plant Biol 151:1609–1616
2. Stortz CA (2006) Carbohydr Res 341:2531–2542
3. Stortz CA (2005) In: Yarema KJ (ed) In: Handbook of carbohydrate engineering. Taylor and Francis, Boca Raton, pp 211–245
4. Campo VL, Kawano DF, da Silva DB Jr, Carvalho I (2009) Carbohydr Polymers 77:167–180
5. Strati GL, Willett JL, Momany FA (2002) Carbohydr Res 337:1851–1859
6. Navarro DA, Stortz CA (2003) Carbohydr Res 338:2111–2118
7. Le Questel JY, Cros S, Mackie W, Perez S (1995) Int J Biol Macromol 17:161–175
8. Parra E, Caro HN, Jimènez-Barbero J, Martin-Lomas M, Bernabé M (1990) Carbohydr Res 208:83–92
9. Urbani R, Di Blas A, Cesàro A (1993) Int J Biol Macromol 15:24–29
10. Ueda K, Ochiai H, Imamura A, Nakagawa S (1995) Bull Chem Soc Jpn 68:95–106
11. Ueda K, Brady JW (1996) Biopolymers 38:461–469
12. Stortz CA, Cerezo AS (2000) J Carbohydr Chem 19:1115–1130
13. Stortz CA, Cerezo AS (1994) J Carbohydr Chem 13:235
14. Stortz CA, Cerezo AS (1995) An Asoc Quim Argent 83:171–181
15. Stortz CA, Cerezo AS (1998) J Carbohydr Chem 17:1405–1419
16. Stortz CA (1999) Carbohydr Res 322:77–86
17. Ragazzi M, Ferro D, Provasoli A (1986) J Comput Chem 7:105–112
18. Ferro DR, Pumilia P, Cassinari A, Ragazzi M (1995) Int J Biol Macromol 17:131–136
19. Huige CJM, Altona C (1995) J Comput Chem 16:56–79
20. Ferro DR, Pumilia P, Ragazzi M (1997) J Comput Chem 18:351–367
21. Lamba D, Glover S, Mackie W, Rashid A, Sheldrick B, Pérez S (1994) Glycobiology 4:151–163
22. Ueda K, Saiki M, Brady JW (2001) J Phys Chem B 105:8629–8638
23. Ueda K, Iwama K, Nakayama H (2001) Bull Chem Soc Jpn 74:2269–2277
24. Schnupf U, Willett JL, Bosma WB, Momany FA (2007) Carbohydr Res 342:2270–2285
25. Ha SN, Madson LJ, Brady JW (1988) Biopolymers 27:1927–1952
26. Tran V, Buleon A, Imberty A, Pérez S (1989) Biopolymers 28:679–690
27. Dowd MK, Zeng J, French AD, Reilly PJ (1992) Carbohydr Res 230:223–244
28. Kouwijzer MLC, Grootenhuis PDJ (1995) J Phys Chem 99:13426–13436

29. Kuttel MM, Naidoo K (2005) J Phys Chem B 109:7468–7474
30. Gould IR, Bettley HA, Bryce RA (2007) J Comput Chem 28:1965–1973
31. Landström J, Widmalm G (2010) Carbohydr Res 345:330–333
32. Hatcher E, Säwén E, Widmalm G, MacKerell AD Jr (2011) J Phys Chem B 115:597–608
33. Perič-Hassler L, Hansen HS, Baron R, Hünenberger PH (2010) Carbohydr Res 345:1781–1801
34. Stortz CA, Johnson GP, French AD, Csonka GI (2009) Carbohydr Res 344:2217–2228
35. Momany FA, Appell M, Willett JL, Schnupf U, Bosma WB (2006) Carbohydr Res 341:525–537
36. Da Silva CO, Nascimento MAC (2004) Carbohydr Res 339:113–122
37. French AD, Johnson GP, Kelterer AM, Csonka GI (2005) Tetrahedron-Asymmetry 16:577–586
38. Momany FA, Willett JL (2000) J Comput Chem 21:1204–1219
39. Strati GL, Willett JL, Momany FA (2002) Carbohydr Res 337:1833–1849
40. Bosma WB, Appell M, Willett JL, Momany FA (2006) J Mol Struct (THEOCHEM) 776:1–19
41. Bosma WB, Appell M, Willett JL, Momany FA (2006) J Mol Struct (THEOCHEM) 776:13–24
42. Appell M, Strati GL, Willett JL, Momany FA (2004) Carbohydr Res 339:537–551
43. Appell M, Willett JL, Momany FA (2005) Carbohydr Res 340:459–468
44. Schnupf U, Willett JL, Bosma WB, Momany FA (2007) Carbohydr Res 342:196–216
45. Momany FA, Appell MA, Strati GL, Willett JL (2004) Carbohydr Res 339:553–567
46. Hricovini M, Scholtzovà E, Bizik F (2007) Carbohydr Res 342:1350–1356
47. Lii J-H, Ma B, Allinger NL (1999) J Comput Chem 20:1593–1603
48. Tvaroska I, Taravel FR, Utille JP, Carver JP (2002) Carbohydr Res 337:353–367
49. Tissot B, Salpin JY, Martinez M, Gaigeot MP, Daniel R (2006) Carbohydr Res 341:598–609
50. Momany FA, Appell M, Willett JL, Bosma WB (2005) Carbohydr Res 340:1638–1655
51. Pogány P, Kovács A (2009) Carbohydr Res 344:1745–1752
52. Dauchez M, Lagant P, Derreumaux P, Vergoten G, Sekkal M (1994) Spectrochim Acta A Mol Spectrosc 50:105–118
53. Dauchez M, Derreumaux P, Lagant P, Vergoten G, Sekkal M, Legrand P (1994) Spectrochim Acta A Mol Biomol Spectrosc 50:87–104
54. Kuttel JM, Brady W, Naidoo K (2002) J Comput Chem 23:1236–1243
55. Schnupf U, Willett JL, Momany FA (2010) J Comput Chem 31:2087–2097
56. Yousfi N, Sekkal-Rahal M, Sayede A, Springborg M (2010) J Comput Chem 31:1312–1320
57. Gonçalves PFB, Stassen H (2002) J Comput Chem 23:706–714
58. Langella E, Rega N, Improta R, Crescenzi O, Barone B (2002) J Comput Chem 23:650–661
59. Curutchet C, Cramer CJ, Truhlar DG, Ruiz-Lopez MF, Rinaldi D, Orozco M, Luque FJ (2003) J Comput Chem 24:284–297
60. Fattebert JL, Gygi F (2002) J Comput Chem 23:662–666
61. Csonka GI, French AD, Johnson GP, Stortz CA (2009) J Chem Theor Comput 5:679–692
62. Kristyan S, Pulay P (1994) Chem Phys Lett 229:175–180
63. IUPAC-IUB Commission on Biochemical Nomenclature (1971) Arch Biochem Biophys 145:405
64. Arnott S, Scott WE Rees DA, McNab CGA (1974) J Mol Biol 90:253–267
65. Janaswamy S, Chandrasekaran R (2001) Carbohydr Res 335:181–194
66. Janaswamy S, Chandrasekaran R (2002) Carbohydr Res 337:523–535
67. French AD, Dowd MK (1993) J Mol Struct (THEOCHEM) 286:183–201
68. Onsager L (1936) J Am Chem Soc 58:1486–1493
69. Foresman JB, Frisch A (1996) Gaussian94 user's guide. Exploring chemistry with electronic structure methods, 2nd edn. Gaussian, Inc, Pittsburgh
70. Frisch MJ, Trucks GW, Schlegel HB, Scuseria GE, Robb MA, Cheeseman JR, Montgomery JA Jr, Vreven T, Kudin KN, Burant JC, Millam JM, Iyengar SS, Tomasi J, Barone V, Mennucci B, Cossi M, Scalmani G, Rega N, Petersson GA, Nakatsuji H, Hada M, Ehara M, Toyota K, Fukuda R, Hasegawa J, Ishida M, Nakajima T, Honda Y, Kitao O, Nakai H, Klene M, Li X, Knox JE, Hratchian HP, Cross JB, Bakken V, Adamo C, Jaramillo J, Gomperts R, Stratmann RE, Yazyev O, Austin AJ, Cammi R, Pomelli C, Ochterski JW, Ayala PY, Morokuma K, Voth GA, Salvador P, Dannenberg JJ, Zakrzewski VG, Dapprich S, Daniels AD, Strain MC, Farkas O, Malick DK, Rabuck AD, Raghavachari K, Foresman JB, Ortiz JV, Cui Q, Baboul AG, Clifford S, Cioslowski J, Stefanov BB, Liu G, Liashenko A, Piskorz P, Komaromi I, Martin RL, Fox DJ, Keith T, Al-Laham MA, Peng CY, Nanayakkara A, Challacombe M, Gill PMW, Johnson B, Chen W, Wong MW, Gonzalez C, Pople JA (2003) Gaussian 03, Revision D.02. Gaussian, Inc, Pittsburgh, PA
71. Golden Software, Inc (2002) Surface mapping system. Golden Software, Inc. Golden, CO
72. Marchessault RH, Pérez S (1979) Biopolymers 18:2369–2374
73. Navarro DA, Stortz CA (2008) Carbohydr Res 343:2292–2298
74. Engelsen SB, Kocà J, Braccini I, du Hervé PC, Pérez S (1995) Carbohydr Res 276:1–30
75. Dowd MK, French AD, Reilly PJ (1994) Carbohydr Res 264:1–19
76. Wong CHS, Siu FM, Ma NL, Tsang CW (2001) J Mol Struct (THEOCHEM) 536:227–234
77. Lii J-H, Chen K-H, Durkin KA, Allinger NL (2003) J Comput Chem 24:1473–1489
78. Lii J-H, Chen K-H, Allinger NL (2003) J Comput Chem 24:1504–1513
79. Momany FA, Willett JL (2000) Carbohydr Res 326:194–209
80. Momany FA, Willett JL (2000) Carbohydr Res 326:210–226
81. Navarro DA, Stortz CA (2005) Carbohydr Res 340:2030–2038
82. Jeffrey GA (1990) Acta Crystallogr B46:89–103
83. Longchambon F, Gillier-Pandraud H (1977) Acta Crystallogr B32:1822–1826
84. Van Eijck BP, Mooij WTM, Kroon J (2001) J Phys Chem B 105:10573–10578
85. McDonnell C, López O, Murphy P, Fernández Bolanõs JG, Hazell R, Bols M (2004) J Am Chem Soc 126:12374–12385
86. Barone V, Cossi M, Tomasi J (1998) J Comput Chem 19:404–417
87. Rashid A, Mackie W (1992) Carbohydr Res 223:147–155
88. Millane RP, Chandrasekaran R, Arnott S, Dea ICM (1988) Carbohydr Res 182:1–17